Temperature Dependence of the Non-Stokesian Charge Transport in Binary Blends of Ionic Liquids†

Philipp Wachter,‡ Markus Zistler,‡ Christian Schreiner,‡ Matthias Fleischmann,‡ Dirk Gerhard,§ Peter Wasserscheid,§ Joseph Barthel,‡ and Heiner J. Gores*,‡

Institut für Physikalische und Theoretische Chemie der Universität Regensburg, D-93040 Regensburg, Germany, and Institut für Chemische Reaktionstechnik, Friedrich-Alexander-Universität, D-91058 Erlangen-Nürnberg, Germany

A comprehensive characterization of an ionic liquid based electrolyte for dye-sensitized solar cells (DSSC) was performed by determination of triiodide diffusion coefficients, viscosities, specific conductivities, and densities. The observed non-Stokesian transport behavior was ensured by determination of triiodide diffusion coefficients with two independent methods, steady-state cyclic voltammetry at ultramicroelectrodes, and polarization measurements at thin layer cells. The electrolyte, consisting of 1-ethyl-3-methylimidazolium tetrafluoroborate ([EMIM][BF_4]), 1-methyl-3-propylimidazolium iodide ([MPIM][I]), and iodine, was examined at fixed iodine concentration over a broad mixing range with varying ionic liquid molar ratio and over a broad temperature range as well. The triiodide diffusion coefficients and the specific conductivity increase with decreasing [MPIM][I] mole fraction or increasing temperature, caused by decreasing electrolyte viscosity. The Einstein−Stokes ratios strongly increase with increasing [MPIM][I] mole fraction and viscosity and thus do not obey the Einstein−Stokes equation. The magnitude of this strong non-Stokesian behavior decreases with increasing temperature. Additional non-Stokesian behavior was found for [MPIM][I]-rich blends since for these blends the Einstein−Stokes ratios strongly decrease at increasing temperatures and simultaneously decreasing viscosity.

Introduction

The dye-sensitized solar cell (DSSC) has been proposed as a low-cost and high-efficiency alternative to conventional photovoltaic cells by O'Regan and Grätzel[1] in 1991. Since then, research in this field was dramatically enforced due to potential low production costs of DSSCs combined with comparably high energy-conversion efficiencies. At present, efficiencies of more than 10 % can be obtained for DSSCs using electrolytes based on volatile organic solvents.[2] However, the usage of these volatile organic electrolytes seriously limits a large-scale implementation of this technology due to poor long-term stability of the cells and the necessity of a complex sealing process.[3,4] Promising alternatives to organic solvents are room-temperature ionic liquids (ILs) since they offer several unique and favorable features such as negligible vapor pressure, excellent electrochemical and thermal stability, and high intrinsic ionic conductivity.[5−7] Among this class of compounds, most attention is attracted by ILs based on the 1,3-dialkylimidazolium cation,[8] especially by 1-methyl-3-propylimidazolium iodide ([MPIM][I]), a commonly used iodide source in electrolytes for DSSCs. However, the comparably high viscosity of this type of imidazolium IL (e.g., [MPIM][I], 1620 mPa·s at 20 °C)[9] renders physical transport processes significantly slower than in common organic solvent based electrolytes and therefore limits the application of these electrolytes. To decrease viscosity, electrolytes based on a binary mixture of [MPIM][I] and low viscous ILs, such as 1-ethyl-3-methylimidazolium dicyanamide ([EMIM][$N(CN)_2$], 21 mPa·s at 25 °C)[10] or 1-ethyl-3-methylimidazolium thiocyanate ([EMIM][SCN], 21 mPa·s at 25 °C),[11] were tested for application in DSSCs, and good cell performances were reported.[8,11] Another possibility to resolve the problem of high electrolyte viscosity and resulting diffusion limitation may be the selective enhancement of the exchange reaction based diffusion of triiodide,[3,12] which contributes to the overall diffusion exclusively in IL-based electrolytes. The non-Stokesian charge transport resulting from the combination of charge transport by physical diffusion and by charge transfer enables much higher overall diffusion coefficients in ILs than in conventional electrolytes of comparable viscosity. Despite this interesting feature of IL-based electrolytes, there is up to the present only one publication dealing with the observation of non-Stokesian charge transport in DSSC electrolytes over a temperature range similar to the one expected during later practical application of DSSCs.[13]

This study provides a comprehensive characterization of a potential electrolyte system for DSSCs and analysis of the temperature dependence of the observed non-Stokesian charge transport behavior. Triiodide diffusion coefficients, viscosities, specific conductivities, and densities of the system 1-ethyl-3-methylimidazolium tetrafluoroborate ([EMIM][BF_4])/[MPIM][I] with 0.05 mol·L^{-1} I_2 were examined at varying [MPIM][I] mole fraction and over a broad temperature range as well and are reported for the first time.

Experimental Section

Materials. Iodine was obtained from Riedel-de Haën (purity of ≥ 99.8 %). The ILs [MPIM][I] and [EMIM][BF_4] were synthesized according to Wachter et al.[14] NMR data (^{1}H, ^{13}C, ^{11}B, ^{19}F) of all ILs described in this paper do not show any

* Corresponding author. E-mail: heiner.gores@chemie.uni-regensburg.de.
† Part of the special issue "Robin H. Stokes Festschrift".
‡ Institut für Physikalische and Theoretische Chemie der Universität Regensburg.
§ Friedrich-Alexander-Universität.

10.1021/je800480d CCC: $40.75
Published on Web 10/21/2008

impurities. After synthesis, the ILs were dried in high vacuum (10^{-3} Pa). The resulting water contents were controlled by Karl Fischer titration using a DL 18 titrator from Mettler (Giessen, Germany), yielding low water mass fractions of $57 \cdot 10^{-6}$ for [MPIM][I] and $39 \cdot 10^{-6}$ for [EMIM][BF_4].

Viscosity Measurements. Viscosity measurements were conducted under Ar-atmosphere using an MCR 100 rheometer from Anton Paar (Graz, Austria). Temperature control (better than ± 0.02 K) was maintained by a Peltier element. The viscosities given were averaged over the values obtained at shear rates ranging from 10 s^{-1} to 1000 s^{-1}. The estimated uncertainties are in the range of (3 to 5) %.

Conductivity Measurements. Conductivity measurements were carried out with an in-house built symmetrical Wheatstone-bridge, with Wagner earth, resistance decade, and sine generator as described by Wachter et al.[15] The conductivity cells were filled and sealed gastight in a glovebox under Ar-atmosphere and then transferred to the thermostat bath. The applied cells with cell constants in the range from (38 to 91) cm^{-1} were previously calibrated with aqueous KCl solutions. The electrolyte resistances were measured at frequencies of 1.7 kHz, 3.2 kHz, 5.1 kHz, 6.5 kHz, and 7.7 kHz, respectively, and extrapolated to infinite frequency. Temperature control was ensured by using the thermostat assembly which is described in detail in refs 15 and 16. With this assembly, a temperature stability of ± 2 mK was achieved. The temperature of the thermostat bath and simultaneous measurement temperature were monitored using an ASL F-250 MkII thermometer (Automatic Systems Laboratories, Milton Keynes). On the basis of the calibration of the individual measuring cells, the estimated uncertainties of the measured specific conductivities are in the range of (0.2 to 0.4) %.

Diffusion Measurements. Triiodide diffusion coefficients were determined by polarization measurements at thin layer cells (TLCs)[3,17] and steady-state cyclic voltammetry at ultramicroelectrodes (UMEs).[9,14,18,19] A three-electrode setup consisting of a Pt-wire as a pseudo-reference electrode, a second Pt-wire as a counterelectrode, and a Pt-disk UME (Bioanalytical Systems Inc., USA) with a radius of 5 μm as a working electrode was used for steady-state cyclic voltammetry measurements. The measurements at UMEs were performed within a Faraday cage using an IM6 from Zahner (Kronach, Germany). Temperature regulation (better than ± 0.05 K) was ensured by application of an RKS 20 thermostat from LAUDA (Lauda-Königshofen, Germany) and additionally controlled by a temperature sensor within the measuring cell. The TLCs used for polarization measurements are described elsewhere.[9,17,20] Polarization measurements at TLCs were conducted in an RK 8 KP thermostat from LAUDA (Lauda-Königshofen, Germany) using an Autolab PGSTAT30 from ECO Chemie BV (Utrecht, The Netherlands). The constancy of temperature in the thermostat bath was better than ± 0.02 K during the measurement. The measuring cells for both methods were filled inside a glovebox under Ar-atmosphere and sealed gastight. The maximum uncertainties of the diffusion coefficients determined at UMEs are estimated to be below 5 %, and those of diffusion coefficients determined with TLCs are below 13 %.

Density Measurements. Densities of the electrolyte mixtures were determined with the precision densitometer DMA 60/DMA 602 from Anton Paar (Graz, Austria). Temperature control (better than ± 0.02 K) was maintained by an RK 8 KP thermostat from LAUDA and controlled by a temperature sensor close to the measuring cell. The estimated uncertainties of the measured densities are below 0.01 %.

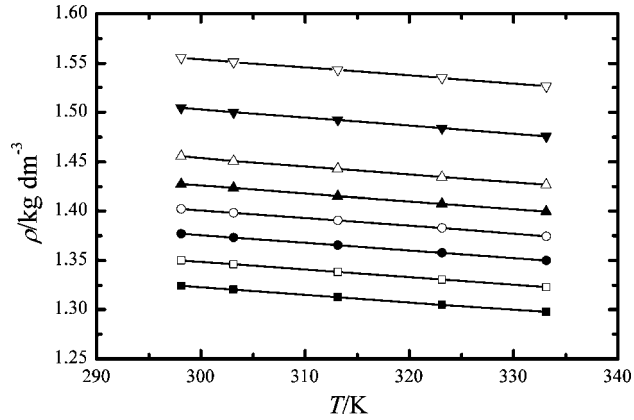

Figure 1. Densities of 0.05 mol·L^{-1} I_2 in mixtures of [EMIM][BF_4]/[MPIM][I] as a function of temperature at varying [MPIM][I] mole fractions x: ■, $x = 0.10$; □, $x = 0.20$; ●, $x = 0.30$; ○, $x = 0.40$; ▲, $x = 0.50$; Δ, $x = 0.60$; ▼, $x = 0.80$; ▽, $x = 1.0$. Continuous lines display results of corresponding quadratic fits.

Table 1. Densities of 0.05 mol·L^{-1} I_2 in Mixtures of [EMIM][BF_4] and [MPIM][I] along with I_2 Molonities $\tilde{m}$ at Varying [MPIM][I] Mole Fractions x

		T/K				
x	$\tilde{m}$/mol·kg^{-1}	298.15	303.15	313.15	323.15	333.15
		ρ/kg·dm^{-3}				
0.10	0.0409	1.3243	1.3204	1.3128	1.3050	1.2975
0.20	0.0376	1.3499	1.3460	1.3384	1.3305	1.3228
0.30	0.0392	1.3769	1.3730	1.3654	1.3576	1.3498
0.40	0.0363	1.4023	1.3983	1.3904	1.3825	1.3746
0.50	0.0329	1.4273	1.4232	1.4153	1.4073	1.3993
0.60	0.0325	1.4557	1.4505	1.4425	1.4344	1.4264
0.80	0.0336	1.5043	1.5002	1.4922	1.4839	1.4757
1.0	0.0315	1.5553	1.5511	1.5430	1.5347	1.5264

Results and Discussion

As shown in refs 13 and 14 the influence of the I_2 concentration on triiodide diffusion is small and depends on a decrease of viscosity with increasing I_2 concentration. High I_2 concentrations in electrolytes for DSSCs also abolish diffusion limitations since the limiting current is proportional to the triiodide concentration as well. However these minor advantages of application of high I_2 concentrations are counterbalanced by enhanced light absorption by the electrolyte and enhanced recombination processes and therefore reduced efficiencies and stabilities.[21] Due to these drawbacks and the negligible influence of increasing I_2 concentration on triiodide diffusion, the system [EMIM][BF_4]/[MPIM][I] was examined with the common standard concentration of 0.05 mol·L^{-1} iodine.

Densities. Exact molar concentrations of the electrolyte's redox-active species are essential for determination of its diffusion coefficient with steady-state cyclic voltammetry at UMEs and polarization measurements at TLCs. Therefore, densities of all blends were determined in the temperature range from (25 to 60) °C.

The measured densities of the blends of the system [EMIM]-[BF_4]/[MPIM][I] with 0.05 mol·L^{-1} I_2 and varying [MPIM][I] mole fractions are given in Table 1 along with the I_2-molonities defined as $\tilde{m}_{solute} = n_{solute}/m_{solution}$. The temperature dependence of the densities was analyzed according to a second-grade polynomial. The resulting quadratic plots and the measured values are shown in Figure 1. The fitting parameters for this system are summarized in Table 2.

Viscosities. A simultaneous determination of viscosities and diffusion coefficients is essential for a complete understanding

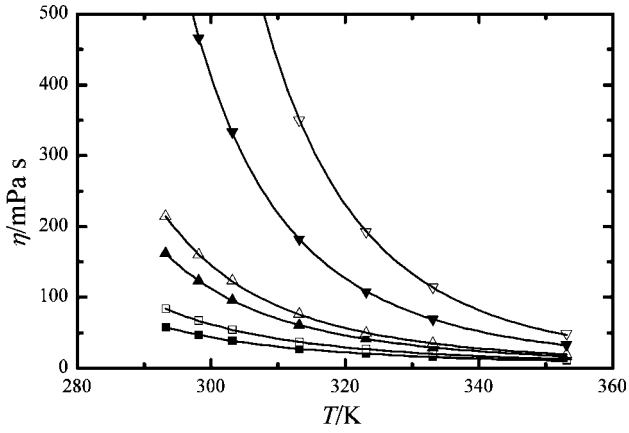

Figure 2. Viscosities of 0.05 mol·L^{-1} I_2 in mixtures of [EMIM][BF_4]/[MPIM][I] as a function of temperature at varying [MPIM][I] mole fractions x: ■, $x = 0.10$; □, $x = 0.20$; ▲, $x = 0.40$; Δ, $x = 0.50$; ▼, $x = 0.80$; ▽, $x = 1.0$. Continuous lines display results of fitting viscosities according to the VFT equation.

Table 2. Density Equation Parameters of 0.05 mol·L^{-1} I_2 in Mixtures of [EMIM][BF_4] and [MPIM][I] as a Function of Temperature at Varying [MPIM][I] Mole Fractions x

	$\rho = k_1 + k_2 \cdot T + k_3 \cdot T^2$			
x	k_1/kg·dm^{-3}	$k_2 \cdot 10^3$/kg·dm^{-3}·K^{-1}	$k_3 \cdot 10^7$/kg·dm^{-3}·K^{-2}	R^2
0.10	1.5652	−0.85	1.255	0.99997
0.20	1.5752	−0.74	−0.5801	0.99996
0.30	1.5801	−0.60	−2.7898	0.99998
0.40	1.6520	−0.88	1.424	0.99999
0.50	1.6603	−0.76	−0.5701	0.99999
0.60	1.9145	−2.18	21.434	0.99933
0.80	1.7222	−0.65	−2.6089	0.99998
1.0	1.7638	−0.59	−3.7558	0.99999

Table 3. Viscosities of 0.05 mol·L^{-1} I_2 in Mixtures of [EMIM][BF_4] and [MPIM][I] at Varying [MPIM][I] Mole Fractions x

	T/K						
x	293.15	298.15	303.15	313.15	323.15	333.15	353.15
	η/mPa·s						
0.10	58	47	39	27	20	16	10
0.20	84	67	54	37	27	20	12
0.40	162	123	96	61	41	29	17
0.50	215	160	123	76	50	35	19
0.80	670	466	333	182	108	69	33
1.0	1535	1023	697	350	192.8	113.9	49.2

of the influence of [MPIM][I] mole fraction on the triiodide diffusion coefficient. Viscosities were determined in the temperature range from (20 to 80) °C. The measured viscosities of the blends of the system [EMIM][BF_4]/[MPIM][I] with 0.05 mol·L^{-1} I_2 and varying [MPIM][I] mole fraction are given in Table 3. The temperature dependence of the recorded viscosities was analyzed by fitting the measurement data according to the Vogel−Fulcher−Tamann (VFT) equation (eq 1)

$$\eta(T) = \eta_0 \exp\left[\frac{B}{T - T_0}\right] \qquad (1)$$

where η_0, B, and T_0 are fitting parameters, and T is the measurement temperature.

The recorded viscosities of the blends of the system [EMIM]-[BF_4]/[MPIM][I] with 0.05 mol·L^{-1} I_2 and varying [MPIM][I] mole fraction and the resulting VFT plots are shown in Figure 2. The fitting parameters of this system are summarized in Table 4. The influence of the [MPIM][I] mole fraction on the viscosity at varying temperatures is displayed in Figure 3. In contrast to the [MPIM][I] mole fraction dependence of the triiodide diffusion coefficients, analyzing the [MPIM][I] mole fraction dependence of the viscosity by means of mathematical expressions was possible. For this purpose, several approaches were examined, and fitting the measurement data according to a fourth-grade polynomial (eq 2) yielded the best results.

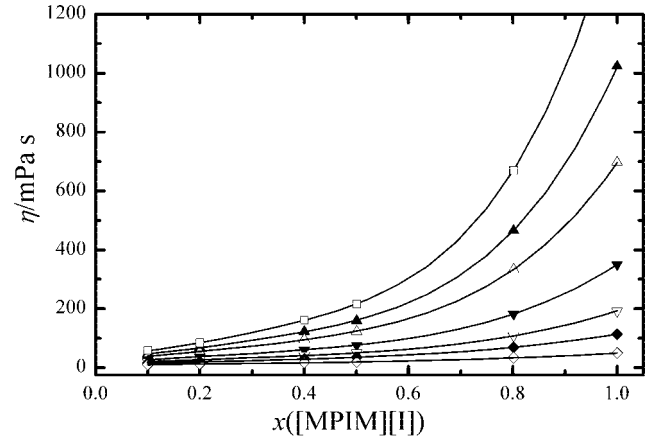

Figure 3. Viscosities of 0.05 mol·L^{-1} I_2 in mixtures of [EMIM][BF_4]/[MPIM][I] as a function of the [MPIM][I] mole fraction x at varying temperatures, T: □, 293.15 K; ▲, 298.15 K; Δ, 303.15 K; ▼, 313.15 K; ▽, 323.15 K; ◆, 333.15 K; ◇, 353.15 K. Continuous lines display results of fitting viscosities according to a fourth-grade polynomial.

Table 4. VFT Equation Parameters of Viscosity Data of 0.05 mol·L^{-1} I_2 in Mixtures of [EMIM][BF_4] and [MPIM][I] at Varying [MPIM][I] Mole Fractions x

x	η_0/mPa·s	B/K	T_0/K	R^2
0.10	0.32808	607.60802	175.763	0.99975
0.20	0.20107	771.39571	165.323	0.99995
0.40	0.17933	811.51156	173.917	0.99997
0.50	0.16191	850.29701	174.899	0.99999
0.80	0.07502	1090.78555	173.252	1
1.0	0.02215	1463.40277	161.866	0.99999

Table 5. Fit Parameters of Fitting Viscosity Data of 0.05 mol·L^{-1} I_2 in Mixtures of [EMIM][BF_4] and [MPIM][I] at Varying Temperatures According to a Fourth-Grade Polynomial

T	A	B_1	B_2	$B_3 \cdot 10^3$	$B_4 \cdot 10^5$	
K	mPa·s	mPa·s	mPa·s	mPa·s	mPa·s	R^2
293.15	45.34308	0.03456	0.14987	−3.28	3.27	1
298.15	32.86266	0.80216	0.07425	−1.73	1.90	1
303.15	27.35164	0.79539	0.04387	−1.0	1.15	0.99999
313.15	16.58528	1.01241	0.00352	−0.191	0.388	0.99999
323.15	11.38392	0.95955	−0.01099	0.0955	0.0999	1
333.15	11.59013	0.47179	−0.00365	0.0517	0.040	1
353.15	7.18889	0.30707	−0.00383	0.0518	−0.00216	0.99973

$$\eta(x) = A + B_1 \cdot x + B_2 \cdot x^2 + B_3 \cdot x^3 + B_4 \cdot x^4 \qquad (2)$$

In eq 2, A, B_1, B_2, B_3, and B_4 are fitting parameters, and x is the [MPIM][I] mole fraction. The resulting plots of fitting the measurement data according to eq 2 are shown in Figure 3 along with the measured values, and the corresponding fitting parameters are listed in Table 5. Since analysis of the viscosity data according to eq 2 yielded good results, interpolation of viscosity values according to eq 2 within the examined mixing range is accurate.

Conductivities. Similar to the viscosity of the blends of the system [EMIM][BF_4]/[MPIM][I], the influence of the [MPIM][I] mole fraction on the specific conductivity was examined as well as its temperature dependence. Therefore, specific conductivities were measured in the temperature range from (5 to 50) °C. The determined specific conductivities at each [MPIM][I] mole fraction and temperature are listed in Table 6. The temperature

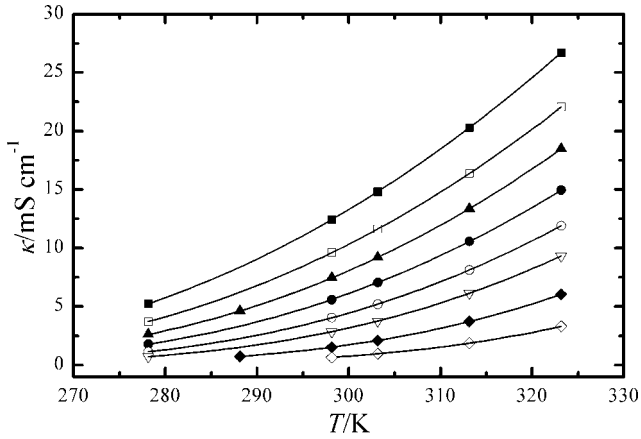

Figure 4. Specific conductivities of 0.05 mol·L^{-1} I_2 in mixtures of [EMIM][BF_4]/[MPIM][I] as a function of temperature at varying [MPIM][I] mole fractions x: ■, $x = 0.10$; □, $x = 0.20$; ▲, $x = 0.30$; ●, $x = 0.40$; ○, $x = 0.50$; ▽, $x = 0.60$; ◆, $x = 0.80$; ◇, $x = 1.0$. Continuous lines display results of fitting conductivities according to the VFT equation.

Table 6. Specific Conductivities of 0.05 mol·L^{-1} I_2 in Mixtures of [EMIM][BF_4] and [MPIM][I] at Varying [MPIM][I] Mole Fractions x

	T/K					
x	278.151	288.152	298.151	303.152	313.150	323.150
	κ/mS·cm^{-1}					
0.10	5.245	-	12.43	14.81	20.29	26.70
0.20	3.720	-	9.600	11.62	16.38	22.05
0.30	2.610	4.620	7.449	9.186	13.37	18.49
0.40	1.782	-	5.595	7.034	10.55	14.95
0.50	1.139	-	4.035	5.194	8.130	11.92
0.60	0.710	-	2.847	3.757	6.134	9.324
0.80	-	0.737	1.523	2.099	3.713	6.035
1.0	-	-	0.656	0.956	1.867	3.306

Table 7. VFT Equation Parameters of Specific Conductivity Data of 0.05 mol·L^{-1} I_2 in Mixtures of [EMIM][BF_4] and [MPIM][I] at Varying [MPIM][I] Mole Fractions x

x	κ_0/mS·cm^{-1}	B/K	T_0/K	R^2
0.10	1410.29461	613.75375	168.43802	1
0.20	1464.65277	634.11132	172.03603	1
0.30	1576.34234	654.44812	175.94363	1
0.40	1568.4225	667.06943	179.77944	1
0.50	1885.6372	718.84175	181.19559	1
0.60	2236.9451	770.48719	182.55327	1
0.80	3510.74583	895.73051	182.44069	1
1.0	4747.98283	997.82907	185.89388	1

dependence of the determined specific conductivities was analyzed by fitting the measurement data according to the VFT equation (eq 3)

$$\kappa(T) = \kappa_0 \exp\left[\frac{-B}{T - T_0}\right] \tag{3}$$

where κ_0, B, and T_0 are fitting parameters.

The resulting VFT plots and the measured values are shown in Figure 4. The fitting parameters for this system are summarized in Table 7. The influence of the [MPIM][I] mole fraction on the specific conductivity at varying temperatures is displayed in Figure 5. The [MPIM][I] mole fraction dependence of the specific conductivity was analyzed according to a fourth-grade polynomial (eq 4)

$$\kappa(x) = A + B_1 \cdot x + B_2 \cdot x^2 + B_3 \cdot x^3 + B_4 \cdot x^4 \tag{4}$$

where A, B_1, B_2, B_3, and B_4 are fitting parameters and x is the [MPIM][I] mole fraction. The resulting plots of fitting the

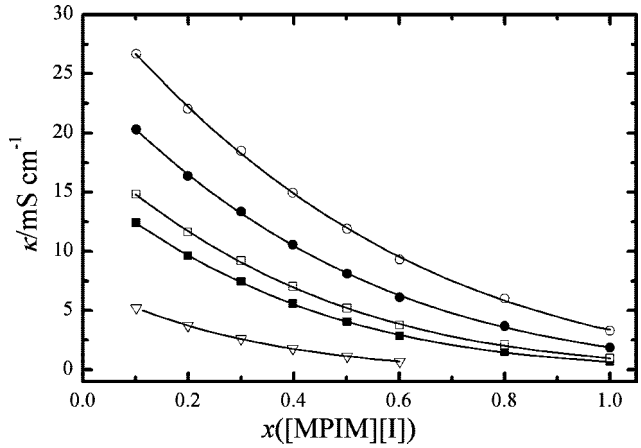

Figure 5. Specific conductivities of 0.05 mol·L^{-1} I_2 in mixtures of [EMIM][BF_4]/[MPIM][I] as a function of the [MPIM][I] mole fraction x at varying temperatures T: ▽, 278.151 K; ■, 298.151 K; □, 303.152 K; ●, 313.150 K; ○, 323.150 K. Continuous lines display results of fitting conductivities according to a fourth-grade polynomial.

Table 8. Fit Parameters of Fitting Conductivity Data of 0.05 mol·L^{-1} I_2 in Mixtures of [EMIM][BF_4] and [MPIM][I] at Varying Temperatures According to a Fourth-Grade Polynomial

T	A	B_1	B_2	B_3·10^5	B_4·10^7	
K	mS·cm^{-1}	mS·cm^{-1}	mS·cm^{-1}	mS·cm^{-1}	mS·cm^{-1}	R^2
278.151	7.49664	−0.26805	0.00504	−6.18	3.47	0.99999
298.151	15.62914	−0.34421	0.00235	0.0162	−0.419	0.9998
303.152	18.33684	−0.37613	0.00222	0.384	−0.585	0.99978
313.150	24.41645	−0.4328	0.00168	1.47	−1.07	0.99974
323.150	31.3762	−0.48399	0.000931	2.76	−1.65	0.99969

Table 9. Triiodide Diffusion Coefficients Determined at UMEs of 0.05 mol·L^{-1} I_2 in Mixtures of [EMIM][BF_4] and [MPIM][I] at Varying [MPIM][I] Mole Fractions x

	T/K				
x	298.15	303.15	313.15	323.15	333.15
	D·10^7/cm^2·s^{-1}				
0.10	3.6	4.4	6.5	8.9	11.6
0.20	3.2	3.9	5.7	8.6	11.6
0.30	3.1	4.0	5.6	8.4	11.9
0.40	2.9	3.8	5.8	8.9	11.7
0.50	2.9	3.7	5.8	8.5	11.8
0.60	2.5	3.3	4.6	7.2	10.6
0.80	1.8	2.5	4.2	7.1	10.4
1.0	1.2	1.7	3.0	4.9	7.4

measurement data according to eq 4 are shown in Figure 5 along with the measured values, and the corresponding fitting parameters are listed in Table 8. Since analysis of the conductivity data according to eq 4 yielded good results, interpolation of specific conductivity values according to eq 4 within the examined mixing range is accurate.

Triiodide Diffusion Coefficients. Triiodide diffusion coefficients were determined with two independent methods. The diffusion coefficients obtained from steady-state cyclic voltammetry at UMEs are listed in Table 9, and the diffusion coefficients from polarization measurements at TLCs are listed in Table 10. The diffusion coefficients determined with UMEs are typically about (5 to 15) % lower than the ones determined at TLCs. However, the influence of temperature and [MPIM][I] mole fraction, respectively, on the diffusion coefficients is nearly identical for the values from both methods. That means for the case of the temperature dependency of the triiodide diffusion coefficients which were determined at UMEs (Figure 6) and with TLCs (Figure 7), there is a strong increase with increasing temperature and decreasing viscosity (Figure 2). Since the VFT

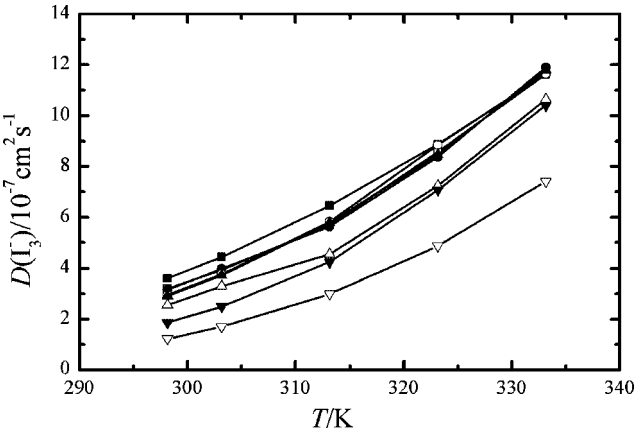

Figure 6. Temperature dependence of I_3^--diffusion coefficients determined with UMEs of 0.05 mol·L^{-1} I_2 in mixtures of [EMIM][BF_4]/[MPIM][I] at varying [MPIM][I] mole fractions x: ■, x = 0.10; □, x = 0.20; ●, x = 0.30; ○, x = 0.40; ▲, x = 0.50; Δ, x = 0.60; ▼, x = 0.80; ▽, x = 1.0. Continuous lines are guides to the eye.

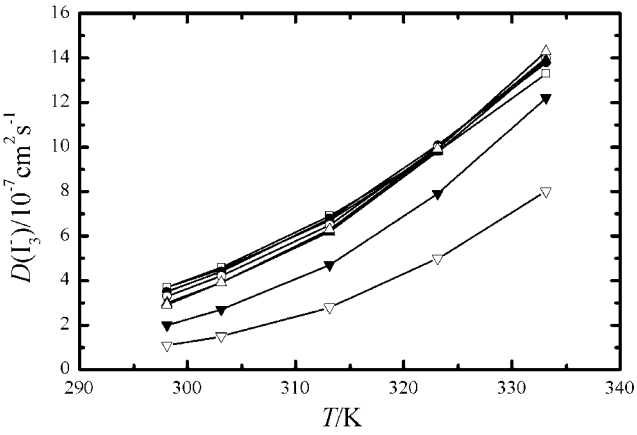

Figure 7. Temperature dependence of I_3^--diffusion coefficients determined with TLCs of 0.05 mol·L^{-1} I_2 in mixtures of [EMIM][BF_4]/[MPIM][I] at varying [MPIM][I] mole fractions x: ■, x = 0.10; □, x = 0.20; ●, x = 0.30; ○, x = 0.40; ▲, x = 0.50; Δ, x = 0.60; ▼, x = 0.80; ▽, x = 1.0. Continuous lines are guides to the eye.

Table 10. Triiodide Diffusion Coefficients Determined at TLCs of 0.05 mol·L^{-1} I_2 in Mixtures of [EMIM][BF_4] and [MPIM][I] at Varying [MPIM][I] Mole Fractions x

	T/K				
x	298.15	303.15	313.15	323.15	333.15
	$D\cdot10^7$/cm$^2\cdot$s^{-1}				
0.10	3.7	4.5	6.7	9.8	13.3
0.20	3.7	4.6	6.9	9.8	13.3
0.30	3.5	4.4	6.8	10.1	13.8
0.40	3.3	4.2	6.5	10.0	14.0
0.50	3.0	3.9	6.2	9.8	13.9
0.60	2.9	3.9	6.3	9.9	14.3
0.80	2.0	2.7	4.7	7.9	12.2
1.0	1.1	1.5	2.8	5.0	8.0

theory was introduced for temperature dependence of viscosity, rigorous analysis of diffusion coefficients according to the VFT equation is only valid if non-Stokesian behavior can be excluded. Thus, analysis of the temperature dependence of the triiodide diffusion coefficients according to the VFT equation was not performed.

The [MPIM][I] mole fraction dependence of the triiodide diffusion coefficients is shown in Figure 8 for diffusion coefficients determined at UMEs and in Figure 9 for those determined with TLCs. Despite a continuously decreasing viscosity with decreasing [MPIM][I] mole fraction (Figure 3), triiodide

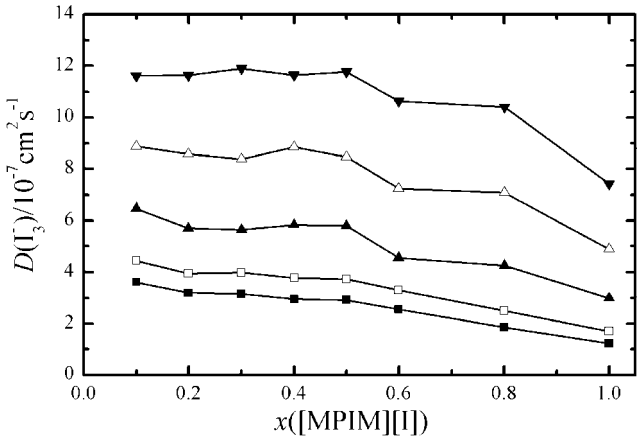

Figure 8. I_3^--diffusion coefficients determined with UMEs of 0.05 mol·L^{-1} I_2 in mixtures of [EMIM][BF_4]/[MPIM][I] as a function of the [MPIM][I] mole fraction x at different temperatures; T: ■, 298.15 K; □, 303.15 K; ▲, 313.15 K; Δ, 323.15 K; ▼, 333.15 K. Continuous lines are guides to the eye.

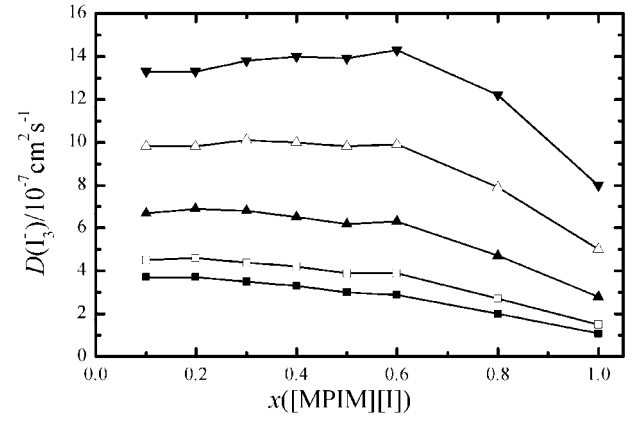

Figure 9. I_3^--diffusion coefficients determined with TLCs of 0.05 mol·L^{-1} I_2 in mixtures of [EMIM][BF_4]/[MPIM][I] as a function of the [MPIM][I] mole fraction x at different temperatures; T: ■, 298.15 K; □, 303.15 K; ▲, 313.15 K; Δ, 323.15 K; ▼, 333.15 K. Continuous lines are guides to the eye.

diffusion coefficients stay nearly constant over a broad mixing range and even show maximum values at higher temperatures and rather high [MPIM][I] mole fractions. This behavior is in clear contrast to the results previously reported[13,22] for triiodide diffusion coefficients in two IL-based DSSC electrolyte systems.

Non-Stokesian Charge Transport. On the basis of the friction force[23,24] for moving spheres in viscous media

$$\vec{F}_r = 6\pi\eta R\vec{v} \tag{5}$$

where η is the viscosity of the liquid; R is the radius of the sphere; and $\vec{v}$ is the velocity of the sphere, a useful relation can be derived for estimating molar conductivities of electrolytes in infinitely dilute solutions at constant temperature Λ_i^∞ (Walden rule)[25] in two solvents of different viscosity

$$\Lambda_1^\infty\eta_1 = \Lambda_2^\infty\eta_2 \tag{6}$$

On the basis of the Einstein−Stokes equation[25,26] (eq 7), where k_B is the Boltzmann constant, a similar relation can be derived for the diffusion coefficient. This so-called Einstein−Stokes ratio (eq 8) should be constant at constant temperatures as well. If this requirement is observed, a Stokesian behavior exists.[25,27,28]

$$D = \frac{k_B T}{6\pi\eta R} \quad (7)$$

$$\frac{D\eta}{T} = \text{const.} \quad (8)$$

The first deviation from this Stokesian behavior reported in the literature was the high mobility of protons in water, for which an alternative transport mechanism was proposed by Grotthuss.[29]

Another deviation from the strict Stokesian behavior was found for the triiodide transport in ILs and their binary blends that are often applied as electrolytes in DSSCs. The triiodide diffusion coefficients in these electrolytes are much higher than expected according to recorded viscosity data and calculated Einstein−Stokes ratios. As reason for this enhanced triiodide transport, a mechanism has already been suggested that depends on the assumption that the triiodide transport is created by a combination of an ordinary diffusion process and a Grotthuss-type charge-transfer mechanism.[3,12,30−32] A similar behavior was observed for the triiodide transport along laminar phases in liquid crystals.[33,34] The suggested charge-transfer process for the case of triiodide can be illustrated as follows

$$I_3^- + I^- \rightarrow I^- \cdots I_2 \cdots I^- \rightarrow I^- + I_3^- \quad (9)$$

The length of the actually participating polyiodide chains is not definitely determined up to now, but chain lengths up to five atoms are know from the literature.[33,35]

According to the above-mentioned triiodide transport mechanism, the apparent or overall diffusion coefficient D_{app} can be split in a physical diffusion coefficient D_{phys} based on diffusion and on a diffusion coefficient D_{ex} based on charge transfer[12,36−38]

$$D_{app} = D_{phys} + D_{ex} \quad (10)$$

For the transfer of I_2 from I_3^- to I^-, both ions have to be in close physical proximity to one another. This leads to a kinetic constraint of this transfer, due to the negative charge of both reactants and the resulting energetic disadvantageous transition state. The constraint would be reduced by larger polyiodide chain lengths and the resulting distribution of the negative charge over the whole chain.

The enhanced triiodide transport is typically observed in ILs since a special feature of ILs is the extremely high ion concentration and therefore also high ionic strength. Due to the high ionic strength, the negative charges of the reacting ions are better screened from one another, and the necessary activation energy is reduced. The result of this kinetic salt effect is the facilitated I_2 transfer compared to other media.[12]

As mentioned above, triiodide diffusion coefficients stay nearly constant over a broad mixing range despite a continuously and strongly decreasing viscosity with decreasing [MPIM][I] mole fraction. That already indicates non-Stokesian charge transport which is further confirmed by the Einstein−Stokes ratios displayed in Figure 10. Instead of staying constant, the Einstein−Stokes ratios for this system strongly and continuously increase with increasing [MPIM][I] mole fraction. The magnitude of the growth decreases with rising temperature from 640 % at 25 °C passing 500 % at 40 °C to 360 % at 60 °C. The increase of the Einstein−Stokes ratios with increasing [MPIM][I] mole fraction corresponds to the above-mentioned mechanism because an exchange between I_3^- and I^- is necessary for this kind of charge transport. Larger iodide concentrations raise the chance of a collision between I_3^- and I^- and therefore enhance this kind of transport mechanism. The impact of the charge transfer mechanism on the overall triiodide transport decreases with increasing temperature due to decreasing viscosity and simultaneously increasing physical triiodide diffusion. In Figure 11, the temperature dependence of the Einstein−Stokes ratios is clarified. The magnitude of the decrease of the Einstein−Stokes ratios with increasing temperature as well as the impact of the charge-transfer process on the overall diffusion are largest for the blends with high [MPIM][I] mole fractions.

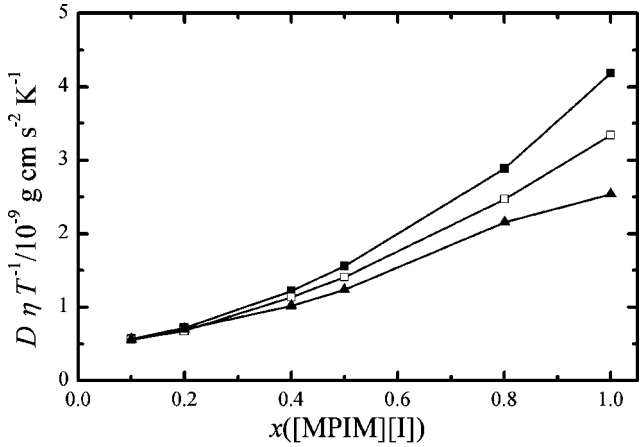

Figure 10. Einstein−Stokes ratios of 0.05 mol·L^{-1} I_2 in mixtures of [EMIM][BF_4]/[MPIM][I] as a function of the [MPIM][I] mole fraction x at different temperatures (calculated with diffusion coefficients determined at UMEs), T: ■, 298.15 K; □, 313.15 K; ▲, 333.15 K. Continuous lines are guides to the eye.

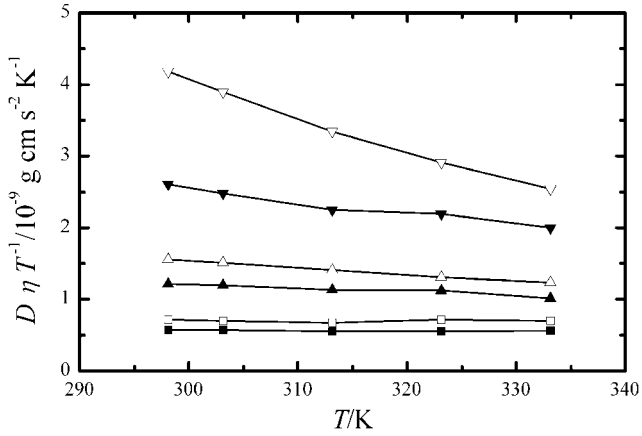

Figure 11. Temperature dependence of Einstein−Stokes ratios of 0.05 mol·L^{-1} I_2 in mixtures of [EMIM][BF_4]/[MPIM][I] at varying [MPIM][I] mole fractions x (calculated with diffusion coefficients determined at UMEs): ■, x = 0.10; □, x = 0.20; ▲, x = 0.40; Δ, x = 0.50; ▼, x = 0.80; ▽, x = 1.0. Continuous lines are guides to the eye.

Conclusion

A comprehensive characterization of an IL-based electrolyte for DSSCs was performed by determination of triiodide diffusion coefficients, viscosities, specific conductivities, and densities. All parameters were examined over a broad [MPIM][I] mole fraction and temperature range. Viscosity and specific conductivity values were accurately correlated with regard to temperature and [MPIM][I] mole fraction. The determined electrolyte densities were analyzed with regard to their temperature dependence as well. The triiodide diffusion coefficient—the predominant electrolyte parameter for limitation of DSSC efficiency—was determined by two independent methods, steady-state cyclic voltammetry at UMEs, and polarization measurements at TLCs. In general, triiodide diffusion coefficients clearly

increase with increasing temperature but only slightly increase with decreasing [MPIM][I] mole fraction, in both cases related to the decreasing electrolyte viscosity. Simultaneous determination of triiodide diffusion coefficients and viscosities enabled a temperature and [MPIM][I] mole fraction dependent analysis of the non-Stokesian charge transport behavior. Instead of staying constant, the Einstein−Stokes ratios strongly increase with increasing [MPIM][I] mole fraction. The magnitude of the growth decreases with rising temperature from 640 % at 25 °C passing 500 % at 40 °C to 360 % at 60 °C. The temperature dependence of this non-Stokesian triiodide transport confirms the assumption of a Grotthuss-type charge transfer mechanism in ILs that occurs in addition to the diffusive charge transport and thus enhances the overall charge transport. Hence, for optimizing an IL-based electrolyte in regards to the triiodide transport, a low electrolyte viscosity is not the exclusive crucial factor since mechanistic transport effects play also an important role to resolve the diffusion limitation of DSSC efficiency.

Acknowledgment

The authors thank Andreas Hinsch of the Fraunhofer Institute for Solar Energy Systems (Freiburg, Germany) for providing the thin-layer cells and R. H. Stokes who paved the way for us to understand electrolyte solutions.

Literature Cited

(1) O'Regan, B.; Grätzel, M. A low-cost, high-efficiency solar cell based on dye-sensitized colloidal TiO_2 films. *Nature* **1991**, *353*, 737–740.
(2) Grätzel, M. Conversion of sunlight to electric power by nanocrystalline dye-sensitized solar cells. *J. Photochem. Photobiol. A* **2004**, *164*, 3–14.
(3) Papageorgiou, N.; Athanassov, Y.; Armand, M.; Bonhôte, P.; Pettersson, H.; Azam, A.; Grätzel, M. The performance and stability of ambient temperature molten salts for solar cell applications. *J. Electrochem. Soc.* **1996**, *143*, 3099–3108.
(4) Hinsch, A.; Kroon, J. M.; Kern, R.; Uhlendorf, I.; Holzbock, J.; Meyer, A.; Ferber, J. Long-term stability of dye-sensitised solar cells. *Prog. Photovoltaics* **2001**, *9*, 425–438.
(5) Wasserscheid, P.; Keim, W. Ionische Flüssigkeiten - innovative Lösungsmittel. *Nachr. Chem.* **2001**, *49*, 12–16.
(6) Buzzeo, M. C.; Evans, R. G.; Compton, R. G. Non-Haloaluminate Room-Temperature Ionic Liquids in Electrochemistry. *ChemPhysChem* **2004**, *5*, 1106–1120.
(7) Galiński, M.; Lewandowski, A.; Stępniak, I. Ionic liquids as electrolytes. *Electrochim. Acta* **2006**, *51*, 5567–5580.
(8) Wang, P.; Zakeeruddin, S. M.; Comte, P.; Exnar, I.; Grätzel, M. Gelation of ionic liquid-based electrolytes with silica nanoparticles for quasi-solid-state dye-sensitized solar cells. *J. Am. Chem. Soc.* **2003**, *125*, 1166–1167.
(9) Zistler, M.; Wachter, P.; Wasserscheid, P.; Gerhard, D.; Hinsch, A.; Sastrawan, R.; Gores, H. J. Comparison of electrochemical methods for triiodide diffusion coefficient measurements and observation of non-Stokesian diffusion behaviour in binary mixtures of two ionic liquids. *Electrochim. Acta* **2006**, *52*, 161–169.
(10) MacFarlane, D. R.; Golding, J.; Forsyth, S.; Forsyth, M.; Deacon, G. B. Low viscosity ionic liquids based on organic salts of the dicyanamide anion. *Chem. Commun.* **2001**, 1430–1431.
(11) Wang, P.; Zakeeruddin, S. M.; Humphry-Baker, R.; Grätzel, M. A binary ionic liquid electrolyte to achieve ≥7% power conversion efficiencies in dye-sensitized solar cells. *Chem. Mater.* **2004**, *16*, 2694–2696.
(12) Kawano, R.; Watanabe, M. Anomaly of charge transport of an iodide/triiodide redox couple in an ionic liquid and its importance in dye-sensitized solar cells. *Chem. Commun.* **2005**, 2107–2109.
(13) Wachter, P.; Zistler, M.; Schreiner, C.; Berginc, M.; Krašovec, U. O.; Gerhard, D.; Wasserscheid, P.; Hinsch, A.; Gores, H. J. Characterization of DSSC-electrolytes based on 1-ethyl-3-methylimidazolium dicyanamide: Measurement of triiodide diffusion coefficient, viscosity, and photovoltaic performance. *J. Photochem. Photobiol. A* **2008**, *197*, 25–33.
(14) Wachter, P.; Schreiner, C.; Zistler, M.; Gerhard, D.; Wasserscheid, P.; Gores, H. J. A microelectrode study of triiodide diffusion coefficients in mixtures of room temperature ionic liquids, useful for dye-sensitised solar cells. *Microchim. Acta* **2008**, *160*, 125–133.
(15) Wachter, R.; Barthel, J. Untersuchungen zur Temperaturabhängigkeit der Eigenschaften von Elektrolytlösungen II. Bestimmung der Leitfähigkeit über einen groβen Temperaturbereich. *Ber. Bunsenges. Phys. Chem.* **1979**, *83*, 634–642.
(16) Barthel, J.; Wachter, R.; Gores, H. J. Temperature Dependence of Conductance of Electrolytes in Nonaqueous Solutions. In *Modern Aspects of Electrochemistry*; Conway, B. E.; Bockris, J. O'M., Eds.; Plenum: New York, 1979; Vol. 13, Chapter 1.
(17) Hauch, A.; Georg, A. Diffusion in the electrolyte and charge-transfer reaction at the platinum electrode in dye-sensitized solar cells. *Electrochim. Acta* **2001**, *46*, 3457–3466.
(18) Baur, J. E.; Wightman, R. M. Diffusion coefficients determined with microelectrodes. *J. Electroanal. Chem.* **1991**, *305*, 73–81.
(19) Ferreira, T. L.; El Seoud, O. A.; Bertotti, M. A microelectrode voltammetric study of the diffusion of CTABr aggregates in aqueous solutions. *Electrochim. Acta* **2004**, *50*, 1065–1070.
(20) Zistler, M.; Wachter, P.; Schreiner, C.; Fleischmann, M.; Gerhard, D.; Wasserscheid, P.; Hinsch, A.; Gores, H. J. Temperature Dependent Impedance Analysis of Binary Ionic Liquid Electrolytes for Dye-Sensitized Solar Cells. *J. Electrochem. Soc.* **2007**, *154*, B925–B930.
(21) Kawano, R.; Matsui, H.; Matsuyama, C.; Sato, A.; Susan, M. A. B. H.; Tanabe, N.; Watanabe, M. High performance dye-sensitized solar cells using ionic liquids as their electrolytes. *J. Photochem. Photobiol. A* **2004**, *164*, 87–92.
(22) Wang, P.; Wenger, B.; Humphry-Baker, R.; Moser, J.-E.; Teuscher, J.; Kantlehner, W.; Mezger, J.; Stoyanov, E. V.; Zakeeruddin, S. M.; Grätzel, M. Charge Separation and Efficient Light Energy Conversion in Sensitized Mesoscopic Solar Cells Based on Binary Ionic Liquids. *J. Am. Chem. Soc.* **2005**, *127*, 6850–6856.
(23) Oseen, C. W. *Hydrodynamik*; Akademische Verlagsgesellschaft: Leipzig, 1927.
(24) Falkenhagen, H. *Theorie der Elektrolyte*; S. Hirzel Verlag: Stuttgart, 1972.
(25) Robinson, R. A.; Stokes, R. H. *Electrolyte Solutions*; Butterworths: London, 1959.
(26) Atkins, P. W. *Physikalische Chemie*; VCH: Weinheim, 1996.
(27) Robinson, R. A.; Stokes, R. H. Solutions of Electrolytes and Diffusion in Liquids. *Annu. Rev. Phys. Chem.* **1957**, *8*, 37–54.
(28) Hanson, H. J.; Tobias, C. W. Electrochemistry of Iodide in Propylene Carbonate I. Cyclic Voltammetry Monitored by Optical Spectroscopy. *J. Electrochem. Soc.* **1987**, *134*, 2204–2210.
(29) de Grotthuss, C. F. T. Sur la décomposition de l'eau et des corps qu'elle tient en dissolution à l'aide de l'électricité galvanique. *Ann. Chim.* **1806**, *58*, 54–73.
(30) Bearcroft, D. J.; Nachtrieb, N. H. Electrical Conductance of Salts in Liquid Iodine. I. Iodide Donor Solutes. *J. Phys. Chem.* **1967**, *71*, 316–323.
(31) Bargeman, D.; Kommandeur, J. Ionic Conductivity in Single Crystals of Iodine: Ions in Iodine. *J. Chem. Phys.* **1968**, *49*, 4069–4082.
(32) Stegemann, H.; Rohde, A.; Reiche, A.; Schnittke, A.; Füllbier, H. Room Temperature Molten Polyiodides. *Electrochim. Acta* **1992**, *37*, 379–383.
(33) Yamanaka, N.; Kawano, R.; Kubo, W.; Kitamura, T.; Wada, Y.; Watanabe, M.; Yanagida, S. Dye-Sensitized TiO_2 Solar Cells Using Imidazolium-Type Ionic Liquid Crystal Systems as Effective Electrolytes. *J. Phys. Chem. B* **2007**, *111*, 4763–4769.
(34) Yamanaka, N.; Kawano, R.; Kubo, W.; Kitamura, T.; Wada, Y.; Watanabe, M.; Yanagida, S. Ionic liquid crystal as a hole transport layer of dye-sensitized solar cells. *Chem. Commun.* **2005**, 740–742.
(35) Kubo, W.; Murakoshi, K.; Kitamura, T.; Yoshida, S.; Haruki, M.; Hanabusa, K.; Shirai, H.; Wada, Y.; Yanagida, S. Quasi-Solid-State Dye-Sensitized TiO_2 Solar Cells: Effective Charge Transport in Mesoporous Space Filled with Gel Electrolytes Containing Iodide and Iodine. *J. Phys. Chem. B* **2001**, *105*, 12809–12815.
(36) Ruff, I.; Friedrich, V. J. J. Transfer diffusion. I. Theoretical. *J. Phys. Chem.* **1971**, *75*, 3297–3302.
(37) Dahms, H. J. Electronic conduction in aqueous solution. *J. Phys. Chem.* **1968**, *72*, 362–364.
(38) Ruff, I.; Botár, L. J. Effect of exchange reactions on transport processes: A comparison of thermodynamic treatment with random walk on lattice points. *J. Chem. Phys.* **1985**, *83*, 1292–1297.

Received for review June 29, 2008. Accepted September 8, 2008. The authors thank the Bundesministerium für Bildung and Forschung (BMBF) under contract No. 01SF0304 for financial support.

JE800480D